

A COMPARATIVE ANALYSIS BETWEEN MODIS LST LEVEL-3 PRODUCT AND IN-SITU TEMPERATURE DATA FOR ESTIMATION OF URBAN HEAT ISLAND OF SOFIA

Ivan Yanev¹, Lachezar Filchev²

¹*ESRI Bulgaria, Ltd., Sofia, Bulgaria*

²*Space Research and Technology Institute – Bulgarian Academy of Sciences
e-mail: ivan.yanevmail@gmail.com*

Abstract

In present study we use global eight-day MODIS Land Surface Temperature (LST) and Emissivity Level-3 satellite products (MOD11A2 and MYD11A2) with in-situ data from automatic weather stations (AWS) to analyze usability and reliability of satellite derived LST data for Urban Heat Island estimation for the city of Sofia, Bulgaria. In order to achieve the study aim the terrestrial measurements from eight AWS were compared to the extracted pixel values from the MODIS LST Level-3 products. The so formed time-series were averaged to align with MODIS LST Level-3 products and gap-filled using the established relationship between the satellite and terrestrial data. A very strong positive relationship ($R^2 \sim 0.97$ at 95% confidence interval) was found for the eight ground AWS which readings were analyzed on a diurnal and seasonal basis for the year of 2013. It is suggested that the pronounced diurnal and seasonal variations in the trends and correlation between satellite and in situ temperature data were primarily related to the different land-use/land-cover type of the mixed pixel of MODIS.

1. Introduction

Due to the greenhouse effect and global warming, thermal environment has received a great attention in the recent years which refers not only to the air temperatures, but also the Land Surface Temperatures (LST) [1, 2]. Human settlements and especially, large urban areas significantly modify the environment [3]. The most documented and unquestioned urban climatic effect is the urban influence on the surface temperature exemplified by the urban heat island (UHI) [4]. The urbanization process leads to two essential changes: change of materials covering the surface which influences the solar radiation absorption, and change of the shapes on the surface which influences the air flows [5].

Surface and atmospheric modifications due to urbanization generally lead to a modified thermal climate that is warmer than the surrounding non-urbanized areas – a phenomenon known as UHI [6]. An UHI is the name given to describe the characteristic warmth of both the atmosphere and surfaces in cities (urban

areas) compared to their (non-urbanized) surroundings [7]. The UHI may be atmospheric heat island when it refers to the relative warmth of the atmosphere or surface heat island – relative warmth of the surface temperature.

Urban areas are demonstrating surface roughness and high urban surface heterogeneity in both horizontal and vertical aspect which makes the analysis of UHI extremely difficult [8]. Many factors affect formation and dynamic of urban microclimate – surface type ratio [9–14], buildings density and height [15–17], buildings exposure and materials (especially roofs) [18], urban geometry [19–21], urban surface materials [22], percent and type of the area directly exposed to the sunlight [23–25], industrial activities [26–29], anthropogenic heat injected from the cooling systems and vehicles [30–32], population density etc. [33].

From the reviewed literature it can be concluded that for a successful analysis of the strongly varying 3D urban environment a big number of densely located stations is needed to collect temperature data. In situ data (in particular, permanent meteorological station data) offer high temporal resolution and long-term coverage but lacks spatial detail which makes them insufficient to monitor the spatial extent of the UHI. Mobile observations overcome this limitation to some extent, but do not provide synchronized view over a city, as well as high density measurement networks are costly [25, 34]. Thermal Infra-Red (TIR) imagery has the advantage of providing a time-synchronized dense grid of temperature data over a whole city [35].

Remote sensors acquire the surface temperature directly exposed to the Instantaneous Field Of View (IFOV) [36]. They measure the LST, which is defined as the skin temperature of the surface (grass, roofs, trees, roads etc.) exposed to the satellite sensor [25, 37]. The LST is a widely used parameter to analyze UHI. Obtaining LSTs over extensive terrains was impractical until the advent of satellite thermal sensor. However, acquiring satellite images with high temporal, spatial, and spectral resolutions remains a problem [38].

Although the satellite-derived temperatures and UHIs are a well-documented issue, and a growing number of publications are issued every year on the topic, the low resolution thermal remote sensing products for UHI estimation has not been validated in Bulgaria until present. The city of Sofia has been studied only recently from [3] who used MODIS to analyze surface temperature of urban areas in Central European cities including Sofia. Non-satellite estimates of the Sofia's UHI have been carried out by micro climatologists and urban climatologists on the basis of comparing meteorological data from the city-centre and the vicinity of Sofia. However, no real estimate of the applicability of MODIS LST for the city of Sofia is known to be published elsewhere.

The study aim is to assess the applicability of MODIS LST Level-3 satellite products for estimating UHI of Sofia, Bulgaria. For this purpose the following objectives have been defined: 1) to compare single MODIS LST Level-3 product with Automatic Weather Stations (AWS) near-surface temperatures;

2) to correlate of MODIS LST Level-3 product with AWS near surface temperatures; and 3) to assess the land cover influence on the correlation.

2. Study area

The area of interest is the city of Sofia – the capital and the biggest city of Bulgaria, and the 16th largest city in the EU [39]. It is located in the West part of the country in the central part of the Sofia valley ($\lambda=23^{\circ}19'28.443''\text{E}$, $\varphi=42^{\circ}41'48.492''\text{N}$) which in turn extends from North-West to South-East between Balkan Mountains on the North and the mountains *Viskyar*, *Lyulin*, *Vitosha*, *Lozenska* on the South, the rivers *Slivnishka* and *Gaberska* on the West and to the East it borders with *Vakarel* Mountain. The entire character of the landscape defines the climate of Sofia. According to climate classification adopted in Bulgaria, Sofia falls into temperate continental climate subzone of European continental climate zone [40]. The city of Sofia is constantly growing in population. The official population estimate in 2015 is around 1.3 million people (2011 census) [41]. This is a prerequisite for the presence of more reliable and frequent meteorological data which make Sofia a suitable place for such an investigation.

3. Data description and processing

Satellite data

The eight-day MODIS global LST and Emissivity Level-3 satellite products (MOD11A2 and MYD11A2) for the whole year of 2013 were used in this study. Two MODIS instruments have been launched onboard TERRA (December 18, 1999) and AQUA (May 4, 2002) platforms as part of NASA's Earth Observing System (EOS) project [42]. The TIR observations for both day and night overpasses of MODIS-Terra at $\approx 10:30$ h (descending) and 22:30 h (ascending) and MODIS-Aqua at $\approx 13:30$ h (ascending) and 1:30 h (descending) local solar time are available in both products [43]. Therefore, four observations are available for each day from a combination of the two sensors increasing the quantity of the emissivity and temperature science data over the global land surface due to the increasing number of MODIS observations in clear sky condition. Other strengths of the MODIS instruments are global coverage, high geolocation accuracy, high radiometric and temporal resolution, and accurate calibration in the visible, near-infrared and TIR bands [44].

The eight-day MODIS LST product is the averaged (simple averaging method) LSTs of the MOD11A1 product over eight days. It is constructed through mapping the SDSs of all pixels in MOD11_L2 products onto grids and averaging the values in each grid. The MODIS LST Level 3, version 5 products are in Sinusoidal projection [8]. A tile contains grids in 1200 rows \times 1200 columns.

The exact grid size at 1 km spatial resolution is 0.928 km×0.928 km. As ϕ increases beyond $\pm 30^\circ$, the LST value at some grids in the MOD11A1 product may be the average value of LSTs retrieved from multiple MODIS observations in clear-sky conditions in day or night. The (MOD11_L2) LST Level 2 product is generated by the generalized split-window LST algorithm [45] and the emissivity in bands 31 and 32 are estimated by the classification-based emissivity method [46]. The LST retrieval in a MODIS swath is constrained to pixels that: 1) have nominal Level 1B radiance data, 2) are in clear-sky conditions at a 99% confidence defined in MOD35, 3) are on land or inland water [8]. According to MODIS land validation web-site MODIS MOD11 (Terra) and MYD11 (Aqua) Collection 5 (C5) has accuracy ≤ 1 K (0.5 K mainly) [47].

Meteorological data

We used daily temperature data for the same time period from automatic weather stations (AWS) available in Weather Underground. This is the first Internet weather service delivering meteorological information globally since 1993 [48]. According to the Weather Underground web-site, the stations are put to a strict quality control. The used raw data from eight AWS, which refer to the entire 2013 year, serve for our diurnal and seasonal dynamic investigation. The 2013 was chosen as it is the most recent year excluding 2014 that was too rainy, i.e. with more cloud cover which limit the availability of MODIS LST product. The AWSs are situated in an urban environment on roof tops or grass areas, Table 1. They collect data in five-minute intervals except AWS *Sofia Airport* which collects its data on an hourly basis. The stations are regularly distributed across the city of Sofia ranging in elevation from 600 to 900 m a.s.l.

Data processing

As the MODIS LST Level-3 product is geometrically, atmospherically, and emissivity corrected, the only pre-processing step that we have applied are a scale factor to the data and a conversion of Kelvin's temperature to degree Celsius. As the MOD11A2 contains eight-day daily and nightly data there were a total of four observations per interception. They were additionally averaged in order to combine TERRA and AQUA MODIS LST Level-3 product and to get more accurate average daily temperature. The task was done by simple averaging method. If one of the four observations was missing we have considered the average value as 'NoData'. There are a total of 46 eight-day MODIS LST scenes (the last one of the yearly time-series is not an eight-day, but five-day average) for 2013. Therefore, we have applied the same averaging method to get the averaged *in-situ* values for the same eight-day interceptions. If more than 3 days for an interception were missing we have considered the average value as 'NoData'.

Table 1. Description of Automatic Meteorological Stations (AWSs) used in the study

AWS name	Data Collection (min)	Latitude (ϕ°)	Longitude (λ°)	Height (m a.s.l.)	AWS Land Cover	MODIS Pixel Land Cover (%)
<i>Sofia Airport</i>	60 min	42.65	23.38	595	Bare ground	100% 'Tall buildings'
<i>Simeonovo</i>	5 min	42.63	23.34	697	Unknown	50 % 'Developed' 50 % 'Bare ground'
<i>Yavorov</i>	5 min	42.69	23.35	554	Unknown	70 % 'Developed' 30 % 'Forest'
<i>Kazichene</i>	5 min	42.66	23.47	542	Tiled roof	75% 'Density houses' 25 % 'Bare ground'
<i>Bistritsa</i>	5 min	42.58	23.37	881	Unknown	100 % 'Bare Ground'
<i>Boyana</i>	5 min	42.64	23.28	744	Unknown	40 % 'Developed' 60 % 'Thick forest'
<i>Manastirski livadi</i>	5 min	42.66	23.28	632	Unknown	70 % 'Developed' 30 % 'Bare ground'
<i>Lyulin</i>	5 min	42.71	23.25	588	Unknown	70 % 'Tall buildings' 30 % 'Bare ground'

There are gaps in the MODIS LST data due to the cloud cover, especially in the winter months. This necessitates filling in the missing values. We have examined two methods to do that by regression equation. The first one considers each MODIS LST observation separately. An independent regression equation has been used to fill the gaps in day/night MODIS TERRA or AQUA LST observations. After that a simple averaging method has been used to extract the average temperatures for each intercept. In the second method we have firstly averaged the different MODIS LST observations and if one of the fourth MODIS LST values has been missing we have assigned 'No Data'. After that the missing values were recovered through a regression equation.

Statistical measures such as: coefficient of determination (R^2), Coefficient of Correlation, Mean Absolute Error (MAE), Root Mean Squared Error (RMSE), and Standard Deviation (SD) were used to compare the so formed two time-series data sets (one terrestrial AWS and one space-borne MODIS LST). As there were gaps in both MODIS LST and AWSs data we have used a regression equation to fill in these gaps. The MODIS LST product with the AWSs' measurements was statistically compared in two ways. Firstly, we have compared the MODIS LST with averaged daily *in-situ* temperature using descriptive statistics. Secondly, we have compared MODIS LST with the *in-situ* data that correspond to the MODIS day-and-night observations.

4. Results and discussions

Comparing single MODIS LST Level-3 product with AWS near surface temperatures

Between the *in-situ* measurements and the MODIS TERRA and AQUA day and night LST observations a correlation was studied. From the visual comparison of Fig. 1, it is obvious that there is strong correlation between AWS *Sofia Airport* and each of MODIS LST observations. However, there are differences in the absolute values. The night time trend lines are closer to AWS trend line than the day time trend lines. Considering day time trend lines a seasonal variation is observed.

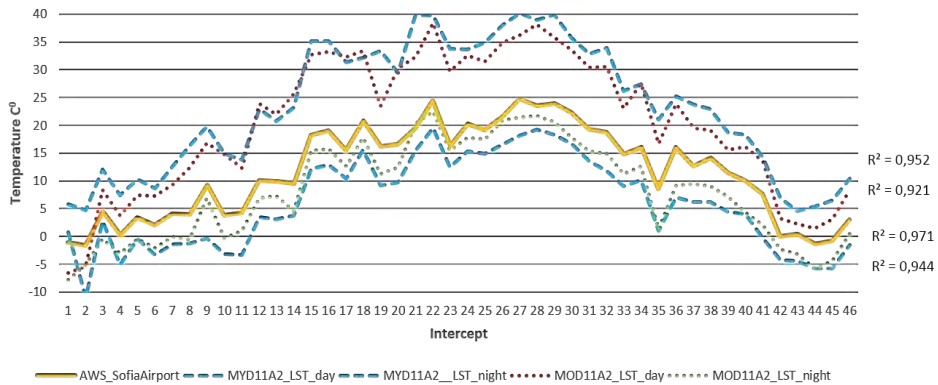


Fig. 1. Comparing temperature measurements (AWS *Sofia Airport*) with eight-day MODIS LST observations for 2013

Averaging MODIS LST level-3 product

As the trend lines from both 1st and 2nd averaging method are almost identical on the plot, the Table 2 shows the results from 1st method leads to slightly more accurate results.

Table 2. Statistical comparison of the two gap-filling methods

MODIS LST averaging after	1 st method	2 nd method
R ²	0.980	0.979
MAE	2.816	2.892
RMSE	3.534	3.565
SD (95% confidence)	4.271	4.169



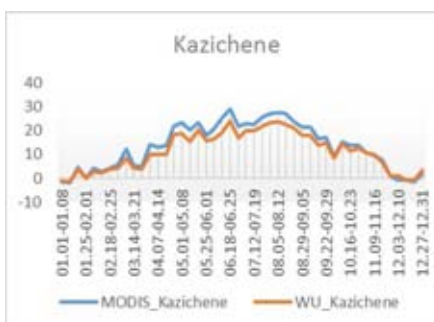
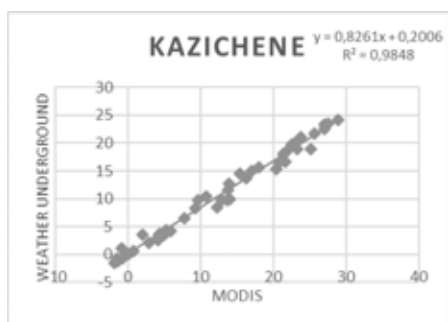
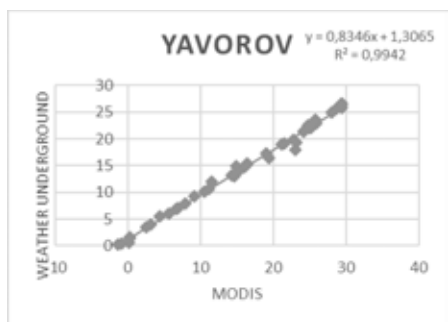
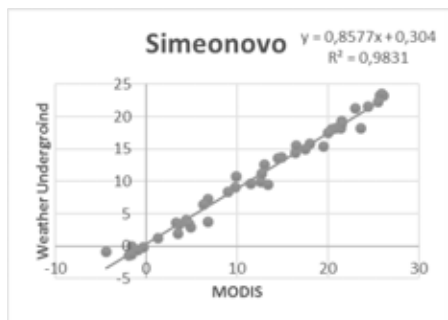
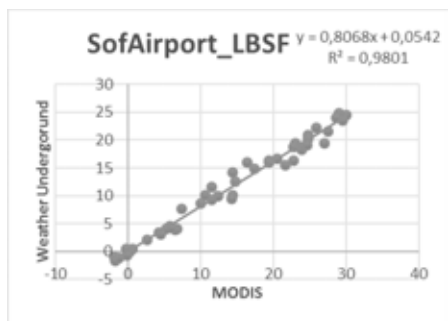
Fig. 2. Comparing AWS Sofia Airport in-situ near-surface temperature observations with averaged MODIS LST observations after the 1st and 2nd method for 2013

Correlation of MODIS LST level-3 product with AWS near-surface temperatures

We have plotted a regression line and trend line for all of the eight AWSs in order to check out the correlation between the two types of data. The correlation coefficient R^2 , among other statistical information, is presented in Table 2.

The MODIS LST Level-3 product has a very strong correlation with all of the AWSs which varies from 0.97 to 0.99. Only AWS *Manastirski livadi* has a value of 0.95. The trend lines moves almost identical in the winter months but in the summer months there is an overestimation from MODIS LST. Exclusions are AWSs *Bistritsa* and *Boyana* where MODIS LST trend line lies on the *in-situ* trend line even in the summer months. These two stations also give the best results. Several statistical parameters have been calculated and are shown in the Table 2. The Mean Bias (which is in fact average T_s – average T_a) is respectively 0.67 and 0.85, the MAE is around 1.1, the RMSE is near 1.4 and SD at 95% confidence is 1.72/1.77. If we divide the results into groups it's apparent the AWSs *Simeonovo*, *Yavorov*, and *Manastirski livadi* have very similar values and the stations *Kazichene* and *Lyulin* form another group with almost identical values. Below this rating is situated AWS *Sofia Airport*. Its Mean Bias is 2.72, the MAE is 2.82, the RMSE – 3.53 and 4.27 SD (95 % confidence). A possible reason for this result is the fact that the MODIS pixel's land-cover is a tall-building area whereas the AWS is located on grassland.

A careful investigation of Fig. 3 confirms our assumption for seasonality in the MODIS LST Level-3 product. In order to check out more carefully this tendency we have analyzed the residuals of MODIS_SofiaAirport data.



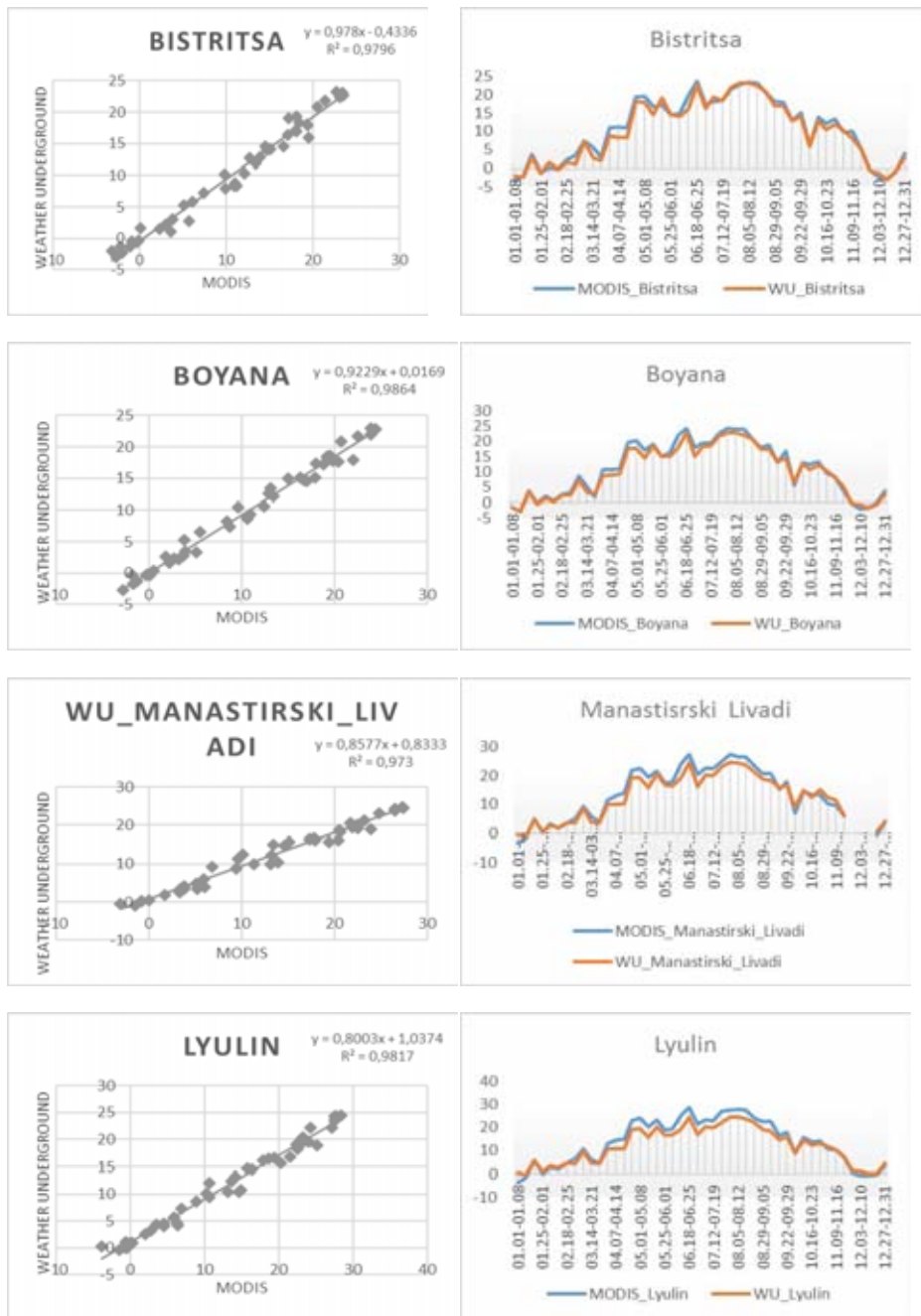


Fig. 3. In-situ (AWS) and MODIS LST regression lines (left) with a comparison of the eight-day time series trends (right) for the eight AWS

Table 3. Descriptive statistics for the AWS data (WU) and MODIS LST pixel values

	MODIS_ Sofia Airport	MODIS_ WU_Sofi Airportvo	MODIS_ Simeono eomovo	MODIS_ WU_Sim Yavorov	MODIS_ WU_Yav orov	MODIS_ WU_Yav Kazichen e	MODIS_ WU_Kaz ichene	MODIS_ WU_Bist ritsa	MODIS_ WU_Bist ritsa	MODIS_ WU_Boy anska	MODIS_ WU_Boyr anski	MODIS_ WU_Liva nastirski	MODIS_ WU_Ma nastirski	MODIS_ WU_Lyul in	MODIS_ WU_Lyu lin
MIN	-1,90	-1,63	-4,37	-1,50	-1,41	0,16	-1,82	-1,50	-3,19	-3,00	-2,81	-2,75	-3,08	-1,00	-3,82
MAX	30,05	24,75	26,14	23,50	29,43	26,63	28,92	24,13	23,57	23,25	24,42	23,00	27,45	24,63	28,45
Absolute MIN difference (Ts-Ta)	0,28		2,87		1,57		0,32		0,19		0,06		2,08		3,45
Absolute MAX difference (Ts-Ta)	5,30		2,64		2,81		4,79		0,32		1,42		2,83		3,95
RZ	0,97		0,97		0,99		0,98		0,97		0,98		0,95		0,97
Mean Bias (Ts-Ta)	2,72		1,44		1,16		2,13		0,67		0,85		1,02		1,68
MAE	2,82		1,80		1,76		2,36		1,06		1,11		1,76		2,27
RMSE	3,53		2,20		2,13		2,87		1,36		1,42		2,12		2,78
SD(99% confidence)	4,27		2,52		2,63		3,26		1,72		1,77		2,49		3,21



Fig. 4. AWS Sofia Airport residual plot

In the first plot on Fig. 4, we have used the near-surface temperature data from AWS *Sofia Airport* for X-axis and the LST data from MODIS pixel at the same location for Y-axis. Until 5 C° the temperatures are underestimated with up to - 2 C° but after this the temperature values of MODIS LST either under or overestimate the real-world ones with ± 2 C°. There could be a tendency for overestimation above 20 C° but these intervals are too small for making general statements. However, the model predicted values are within ± 2 C° for a given observation temperature.

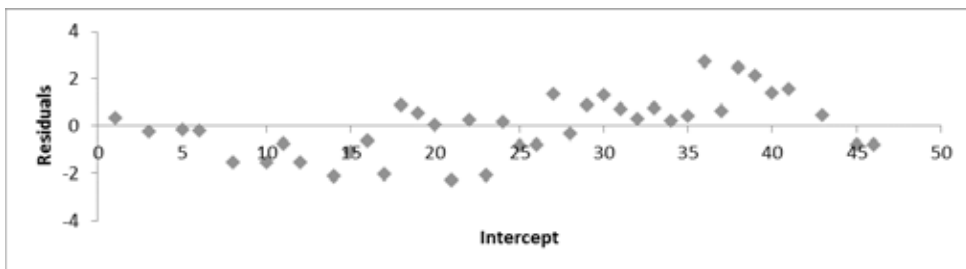


Fig. 5. Intercept residual plot

Observing the second plot on Fig. 5, there are apparently more readable results. This time the intercepts have been plotted on the X-axis. Here it is observed a tendency for a smooth displacement of the predicted values moving through the intercepts. This movement is expressed in underestimation in the winter intercepts, a mixed under- and overestimation in the transitional intercepts, and an overestimation in the summer intercepts.

Land cover influence on the correlation

It is well documented fact that the impervious surfaces raise the LSTs whereas the green/vegetated surfaces lower them [49, 50]. The MODIS LST pixel value is a combination of the thermal properties of all the represented land-cover types [38]. In table 1 we have described the land cover under the MODIS pixels. Comparing the presence of different land cover types to the statistical information in a table 2 it is observed an interesting tendency about the influence of the urban area on the LSTs. Earlier we have combined the statistical results into groups by their rating. A combination of these groups with the pixels' land cover description answers the question about the urban impact on the LST (Table 4).

Table 4. Comparison of statistical groups with pixel land cover types of MODIS LST. The AWS names are encoded from dark grey (worst) to white (best) statistical agreement (in terms of MAE, RMSE, and SD) with MODIS LST values

AWS name	Land use-land-cover class (%)
<i>Sofia Airport</i>	100 % 'Tall buildings'
<i>Simeonovo</i>	50 % 'Developed', 50 % 'Bare ground'
<i>Yavorov</i>	70 % 'Developed', 30 % 'Park'
<i>Kazichene</i>	75 % 'Dense housing with vegetation', 25 % 'Bare ground'
<i>Bistritsa</i>	100 % 'Bare Ground'
<i>Boyana</i>	40 % 'Developed', 60 % 'Thick forest'
<i>Manastirski livadi</i>	70 % 'Developed', 30 % 'Bare ground'
<i>Lyulin</i>	70 % 'Tall buildings', 30 % 'Bare ground'

As we have already stated AWS *Sofia Airport* (dark grey) has the worst statistical result expressed in rising of trend line in summer months and bigger MAE, RMSE, and SD values. The pixel area consists of tall buildings and runways leading to a higher surface temperature. In fact the MODIS LST product measure 5.30°C higher absolute maximum temperature than the AWS *Sofia Airport* (Table 2). The gray group which consists mainly of tall buildings or densely built houses has a slightly better result that may be due to the presence of 25÷30 % bare

ground. The next, pale grey group consists of mix from developed, bare ground, and park areas and the white encoded group, which has the best results, consists of bare ground or prevailing thick forest, i.e. natural formations.

On the other hand, the land cover influences not only the surface temperature, but the air temperature measured by AWSs. Unfortunately, we do not know the precise location of all of the AWSs. Hence, we would not know if a station is on the roof top or on the ground. We only have information for the AWS *Sofia Airport* which is on the ground and AWS *Kazichene* which is on a tiled roof top.

5. Conclusion

A very strong correlation with a pronounced seasonality between MODIS LST Level-3 product and near surface *in-situ* temperature observation exists. The averaged R^2 value is 0.97 with average MAE, RMSE, and SD at 95 % confidence respectively 1.87/2.30/2.73. The results are pronouncedly influenced by the land cover. In fact, the stations with prevailing non-urbanized area have better predicted values (MODIS LST) than the stations with mainly impervious surfaces. The trend lines are almost identical in the winter months but take apart in the summer months. The figure 1 shows this trend holds only for day time MODIS LST observations. From the residual plots and table 3 we can state that the driving force for the seasonality is not the increase of temperatures itself but the sunlight in combination with the presence of impervious surfaces. Considering correlation between these two types of temperature measurements another possible factor could be the altitude. However, with the available data we could not find a strong relationship between MODIS and AWS measurements with respect to the elevation, which is to be studied further. Having stated, that we compare surface versus near-surface temperatures, it is possible to have seasonality in the results which may be influenced by many other climatic processes such as advection.

In conclusion, the strong correlation and the low level of MAE, RMSE, and SD prove the applicability of MODIS LST Level-3 product in UHI studies. It could be suggested that such investigations have to study and model first the local cityscapes LSTs and compare with the LST satellite products and only then to analyze their UHIs to allow for a better analysis of local conditions for decision making.

References

1. Zhang, J., Y. Wang, & Y. Li. A C++ program for retrieving land surface temperature from the data of Landsat TM/ETM+ band 6. *Comp. & Geosci.*, 2006, 32(10), 1796–1805. DOI: 10.1016/j.cageo.2006.05.001 (last accessed: 16 March 2017).

2. Falahatkar, S., S.M. Hosseini, & A. Reza. The relationship between land cover changes and spatial-temporal dynamics of land surface temperature. *Indian J. for Sci. and Tech.*, 2011, 4(2), 76–81. DOI: 10.17485/ijst 2011/v4i2/29937
3. Pongrácz, R., J. Bartholy, & Z. Dezso. Application of remotely sensed thermal information to urban climatology of Central European cities. *Physics and Chemistry of the Earth*, 2010, 35(1–2), 95–99. DOI: 10.1016/j.pce.2010.03.004
4. Atwater, M.A. Thermal changes induced by urbanization and pollutants. *J. of Applied Meteor.*, 1975, 14, 1061–71. DOI: 10.1175/1520-0450(1975)014%3C1061:TCIBUA%3E2.0.CO;2 (last date accessed: 21 December 2016).
5. Ojima, T. Changing Tokyo Metropolitan area and its heat island model. *Energy and Buildings*, 1990, 15(1–2), 191–203. DOI: 10.1016/0378-7788(90)90131-2
6. Voogt, J.A. & T.R. Oke. Thermal remote sensing of urban climates. *Rem. Sens. of Environ.*, 2003, 86(3), 370–384. DOI: 10.1016/S0034-4257(03)00079-8
7. Voogt, J.A. Urban heat islands: hotter cities. *Actionbioscience*. 2004, URL: <http://www.actionbioscience.org/environment/voogt.html>
8. Arnfield, A.J. Two decades of urban climate research: A review of turbulence, exchanges of energy and water, and the urban heat island. *Int. J. of Climatology*, 2003, 23(1), 1–26. DOI: 10.1002/joc.859 (last date accessed: 21 December 2016).
9. Moriyama, M. Estimation of land cover ratio using remote sensing data (LANDSAT MSS) for investigating thermal properties of urban areas. *Energy and Buildings*, 1990, 15(C), 177–181. DOI: 10.1016/0378-7788(90)90129-7
10. Wan, Z. Collection 5 MODIS Land Surface Temperature Products Users' Guide, 2006. http://www.ices.ucsb.edu/modis/LstUsrGuide/MODIS_LST_products_Users_guide_C5.pdf (last date accessed: 21 December 2016).
11. Huang, G., W. Zhou, & M.L. Cadenasso. Understanding the relationship between urban land surface temperature, landscape heterogeneity and social structure. In: 30th IEEE International Geoscience and Remote Sensing Symposium, IGARSS 2010. Center for Regional Change, University of California, Davis, USA, 2010, 3933–36. DOI: 10.1109/IGARSS.2010.5649806 (last date accessed: 21 December 2016).
12. Kottmeier, C., C. Biegert, & U. Corsmeier. Effects of urban land use on surface temperature in Berlin: case study. *J. of Urban Plan. and Develop.*, 2007, 133(2), 128–137. DOI: 10.1061/(ASCE)0733-9488(2007)133:2(128)
13. Rinner, C. & M. Hussain. Toronto's urban heat island-exploring the relationship between land use and surface temperature. *Remote Sensing*, 2011, 3(6), 1251–65.
14. Amiri, R., Q. Weng, A. Alimohammadi, & S.K. Alavipanah. Spatial-temporal dynamics of land surface temperature in relation to fractional vegetation cover and land use/cover in the Tabriz urban area, Iran. *Rem. Sens. of Environ.* 2009, 113(12), 2606–17. DOI: 10.1016/j.rse.2009.07.021
15. Wong, M.S., J.E. Nichol, P.H. To, & J. Wang, A simple method for designation of urban ventilation corridors and its application to urban heat island analysis. *Building and Environment*, 2010, 45(8), 1880–89. DOI: 10.1016/j.buildenv.2010.02.019 (last date accessed: 21 December 2016).
16. Loughner, C.P., J.A. Dale, Z. Da-Lin, K.E. Pickering, R.R. Dickerson, & L. Landry. Roles of Urban Tree Canopy and Buildings in Urban Heat Island Effects: Parameterization and Preliminary Results. *J. of Applied Meteorology and Climatology*, 2012, 51(10), 1775–93. DOI: 10.1175/JAMC-D-11-0228.1

17. Stanganelli, M. & M. Soravia. Connections between urban structure and urban heat island generation: An analysis through remote sensing and GIS. *Lecture Notes in Computer Science (including subseries Lecture Notes in Artificial Intelligence and Lecture Notes in Bioinformatics)*, 2012, 7334 LNCS(PART 2), 599–608. DOI: 10.1007/978-3-642-31075-1_45 (last date accessed: 21 December 2016).
18. Stathopoulou, M., A. Synnefa, C. Cartalis, M. Santamouris, T. Karlessi, & H. Akbari. A surface heat island study of Athens using high-resolution satellite imagery and measurements of the optical and thermal properties of commonly used building and paving materials. *International Journal of Sustainable Energy*, 2009, 28(1–3), 59–76. DOI: 10.1080/14786450802452753 (last accessed: 21 December 2016).
19. Du, M., W. Sun, & G. Cai. Calculation of corridor structure effect on urban heat island using highly spatial resolution satellite images in Beijing, China. In *International Geoscience and Remote Sensing Symposium (IGARSS). 2008 IEEE International Geoscience and Remote Sensing Symposium - Proceedings*. School of Geomatic and Urban Information, Beijing University of Civil Engineering and Architecture, No.1, Zhanlanguan Road, 100044, China, 2008, III1342–III1345. DOI: 10.1109/IGARSS.2008.4779608 (last date accessed: 21 December 2016).
20. Nakata, C.M. & L.C.L. de Souza. Verification of the influence of urban geometry on the nocturnal heat island intensity. *J. of Urban and Environ. Engineering*, 2013, 7(2), 286–292. DOI: 10.4090/juee.2013.v7n2 (last accessed: 21 December 2016).
21. Voogt, J.A. & T.R. Oke. Effects of urban surface geometry on remotely-sensed surface temperature. *International Journal of Remote Sensing*, 1998, 19(5), 895–920. DOI: 10.1080/014311698215784 (last date accessed: 21 December 2016).
22. Di Maria, V., M. Rahman, P. Collins, G. Dondi & C. Sangiorgi. Urban Heat Island effect: thermal response from different types of exposed paved surfaces. *Int. Journal of Pavement Research and Technology*, 2013, 6(4), 414–422. DOI: 10.6135/ijprt.org.tw/2013.6(4).414 (last date accessed: 21 December 2016).
23. Oke, T.R. *Boundary Layer Climates*, Methuen, 1987, 435 p.
24. Gluch, R., D.A. Quattrochi, & J.C. Luvall. A multi-scale approach to urban thermal analysis. *Remote Sensing of Environment*, 2006, 104(2), 123–132. DOI: 10.1016/j.rse.2006.01.025 (last date accessed: 21 December 2016).
25. Voogt, J.A. Assessment of an urban sensor view model for thermal anisotropy. *Rem. Sens. of Environ.*, 2008, 112(2), 482–495. DOI: 10.1016/j.rse.2007.05.013
26. Liu, L. & Y. Zhang. Urban Heat Island analysis using the Landsat TM Data and ASTER data: A case study in Hong Kong. *Rem. Sens.*, 2011, 3(12), 1535–52. DOI: 10.3390/rs3071535 (last date accessed: 21 December 2016).
27. Klok, L., S. Zwart, H. Verhagen & E. Mauri. The surface heat island of Rotterdam and its relationship with urban surface characteristics. *Resources, Conservation and Recycling*, 2012, 64, 23–29. DOI: 10.1016/j.resconrec.2012.01.009
28. Jiang, X., B. Xia, G. Lin & W. Lin. Daily changes of spatial patterns of meteorological elements over Pearl River Delta based on GIS and MM5. *Chin. Geog. Sci.*, 2009, 19(1), 69–76. DOI: 10.1007/s11769-009-0069-1
29. Van, T.T., H. Duong, & X. Bao. A study on urban development through land surface temperature by using remote sensing: in case of Ho Chi Minh City, Southern Vietnam. *Geog. Res.*, 2008, 24, 160–167. DOI: 10.1111/j.1745-5871.2009.00607.x

30. Yang, L. & Y. Li. City ventilation of Hong Kong at no-wind conditions. *Atmos. Environ.*, 2009, 43(19), 3111–21. DOI: 10.1016/j.atmosenv.2009.02.062 (last date accessed: 21 December 2016).
31. Liu, H. & Q. Weng. Seasonal variations in the relationship between landscape pattern and land surface temperature in Indianapolis, USA. *Environ. Monitor. & Assess.*, 2008, 144(1–3), 199–219. DOI: 10.1007/s10661-007-9979-5 (last date accessed: 21 December 2016).
32. Rizwan, A.M., L.Y.C. Dennis, & C. Liu. A review on the generation, determination and mitigation of Urban Heat Island. *J. of Environ. Sci.*, 2008, 20(1), 120–128. DOI: 10.1016/S1001-0742(08)60019-4 (last date accessed: 21 December 2016).
33. Mallick, J. & A. Rahman. Impact of population density on the surface temperature and micro-climate of Delhi. *Current Sci.*, 2012, 102(12), 1708–13. URL: <http://www.currentscience.ac.in/Volumes/102/12/1708.pdf>
34. Weng, Q. Thermal infrared remote sensing for urban climate and environmental studies: Methods, applications, and trends. *ISPRS J. of Photogram. and Rem. Sens.*, 2009, 64(4), 335–344. DOI: 10.1016/j.isprsjprs.2009.03.007
35. Steininger, M.K. Tropical secondary forest regrowth in the Amazon: age, area and change estimation with Thematic Mapper data. *Int. J. of Rem. Sens.*, 1996, 17(1), 9–27. DOI: 10.1080/01431169608948984 (last date accessed: 21 December 2016).
36. Soux, A., J.A. Voogt, & T.R. Oke. A model to calculate what a remote sensor “sees” of an urban surface. *Boundary-Layer Meteor.*, 2004, 111(1), 109–132. DOI: 10.1023/B:BOUN.0000027978.21230.b7 (last accessed: 21 December 2016).
37. Qin, Z. & A. Karnieli. Progress in the remote sensing of land surface temperature and ground emissivity using NOAA-AVHRR data. *Int. J. of Rem. Sens.*, 1999, 20(12), 2367–93. DOI: 10.1080/014311699212074 (last accessed: 21 December 2016).
38. Zhan, W., Y. Chen, J. Zhou, J. Wang, W. Liu, J. Voogt, X. Zhu, J. Quan, & J. Li. Disaggregation of remotely sensed land surface temperature: Literature survey, taxonomy, issues, and caveats. *Rem. Sens. of Environ.*, 2013, 131, 119–139. DOI: 10.1016/j.rse.2012.12.014 (last date accessed: 21 December 2016).
39. EUROSTAT – City Statistics Illustrated, 2015. URL: <http://ec.europa.eu/eurostat/cache/RSI/#?vis=city.statistics> (last date accessed: 21 December 2016).
40. Climate guide of People’s Republic of Bulgaria. Volume 3: Air temperature, soil temperature, frost. Sofia, Bulgaria, 1983. (in Bulgarian)
41. National Statistical Institute (NSI). Population by districts, municipalities, settlements and age to 01.02.2011. <http://goo.gl/UXt2pf> (last accessed: 22 December 2016).
42. MODIS (Moderate Resolution Imaging Spectroradiometer). <http://modis.gsfc.nasa.gov/about/design.php> (last date accessed: 15 December 2016).
43. Sohrabinia, M., W. Rack, & P. Zawar-Reza. Analysis of MODIS LST compared with WRF model and in situ data over the Waimakariri river basin, Canterbury, New Zealand. *Rem. Sens.*, 2012, 4(11), 3501–27. DOI: 10.3390/rs4113501
44. Wan, Z., Y. Zhang, Q. Zhang & Z.-L. Li. Quality assessment and validation of the MODIS global land surface temperature. *Int. J. of Rem. Sens.*, 2004, 25(1), 261–274. DOI: 10.1080/0143116031000116417 (last accessed: 21 December 2016).
45. Wan, Z., & J. Dozier. A generalized split-window algorithm for retrieving land-surface temperature from space. *IEEE Transactions on Geosci. and Rem. Sens.*, 1996, 34(4), 892–905. DOI: 10.1109/36.508406 (last date accessed: 22 December 2016).

46. Snyder, W.C., Z. Wan, Y. Zhang, & Y.Z. Feng. Classification-based emissivity for land surface temperature measurement from space. *Int. J. of Rem. Sens.*, 1998, 19(14), 2753–74. DOI: 10.1080/014311698214497 (last accessed: 22 December 2016).
47. MODIS land validation team. URL: <http://landval.gsfc.nasa.gov/ProductStatus.php?ProductID=MOD11> (last date accessed: 15 December 2016).
48. Weather Underground. URL: <http://www.wunderground.com/about/background.asp> (last date accessed: 15 December 2016).
49. Tomlinson, C.J., L. Chapman, J.E. Thornes & C. Baker. Remote sensing land surface temperature for meteorology and climatology: A review. *Meteorological Applications*, 2011, 18(3), 296–306. DOI: 10.1002/met.287
50. Rajasekar, U. & Q. Weng. Urban heat island monitoring and analysis using a non-parametric model: A case study of Indianapolis. *ISPRS J. of Photogram. and Rem. Sens.*, 2009, 64(1), 86–96. DOI: 10.1016/j.isprsjprs.2008.05.002 (last date accessed: 21 December 2016).

СРАВНИТЕЛЕН АНАЛИЗ МЕЖДУ MODIS LST НИВО-3 СПЪТНИКОВИ ПРОДУКТИ И НАЗЕМНИ ТЕМПЕРАТУРНИ ИЗМЕРВАНИЯ ЗА ОЦЕНКА НА ГРАДСКИЯ ТОПЛИНЕН ОСТРОВ НА ГР. СОФИЯ

И. Янев, Л. Филчев

Резюме

В настоящето изследване използваме осемдневни спътникови продукти ниво-3 за глобалната температура на земната повърхност и топлинното излъчване от спътниковия сензор MODIS (MOD11A2 и MYD11A2) и наземни данни от автоматични климатични станции (АКС) за анализиране на пригодността и надеждността на спътниковите данни за оценка на градския топлинен остров на гр. София, България. За целта са сравнени наземни температурни данни от осем АКС с извлечени пикселни стойности от MODIS LST Ниво-3 продукти за 2013 г. Така получената времева серия е осреднена за привеждане в съответствие с MODIS LST Ниво-3 продуктите. Липсващите данни във времевата серия са запълнени с помощта на корелационен анализ между спътниковите и наземни температурни данни. Установена е много силна положителна корелационна зависимост ($R^2 \sim 0.97$ при 95 % доверителен интервал) за осемте АКС, чиито денонощна и сезонна динамика беше анализирана. Изказано е предположението, че добре изразените денонощни и сезонни колебания в температурния тренд и корелацията между спътниковите MODIS LST Ниво-3 продукти и наземни данни, са преди всичко свързани със смесения пиксел от MODIS (с различни типове земеползване/земно-покритие).